Meteoritics & Planetary Science 35, 827–839 (2000)

A new martian meteorite from the Sahara: The shergottite Dar al Gani 489

L. FOLCO[1]*, I. A. FRANCHI[2], M. D'ORAZIO[3], S. ROCCHI[3] AND L. SCHULTZ[4]

[1]Museo Nazionale dell'Antartide, Università di Siena, Via Laterina 8, I-53100 Siena, Italy
[2]Planetary Sciences Research Institute, Open University, Milton Keynes MK7 6AA, U.K.
[3]Dipartimento di Scienze della Terra, Università di Pisa, Via S. Maria 53, I-56126 Pisa, Italy
[4]Max-Planck-Institut für Chemie, Abteilung Kosmochemie, Postfach 3060, D-55020 Mainz, Germany
*Correspondence author's e-mail address: folco@unisi.it

(Received 1999 November 3; accepted in revised form 2000 April 12)

Abstract–Dar al Gani 489 (DaG 489) is a meteorite fragment of 2146 g found in the Libyan Sahara by a meteorite finder during one of his search campaigns in 1997–98. It is a porphyritic rock with millimeter-sized olivine crystals ($Fo_{79–59}$) set in a fine-grained groundmass (average grain size 0.1 mm) consisting of pigeonite ($En_{75–57}$ $Wo_{5–15}$) crystals and interstitial feldspathic glass ($An_{67–56}$ $Or_{0–1}$). Minor phases include enstatite ($En_{82–71}$ $Wo_{2–4}$), augite ($En_{48–52}$ $Wo_{29–32}$), chromite, Ti-chromite, ilmenite, pyrrhotite, merrillite, and secondary calcite and iron oxides. On the basis of mineralogical, petrographic, bulk chemical, O-isotopic, and noble gas data, DaG 489 can be classified as a highly shocked martian meteorite (*e.g.*, $Fe/Mn_{(bulk)}$ = 42.1, $Ni/Mg_{(bulk)}$ = 0.002; $\delta^{17}O$ = 2.89, $\delta^{18}O$ = 4.98, and $\Delta^{17}O$ = 0.305), belonging to the basaltic shergottite subgroup.

The texture and modal composition of DaG 489 are indeed those of basalts; nonetheless, the bulk chemistry, the abundance of large olivine and chromite crystals, and enstatitic pyroxene suggest some relationship with lherzolitic shergottites. As such, DaG 489 is similar to the hybrid shergottite Elephant Moraine (EET) A79001 lithology A; however, there are some relevant differences including a higher olivine content (20 vol%), the lack of orthopyroxene megacrysts, a higher molar $Mg/(Mg + Fe)_{(molar)}$ = 0.68, and a lower rare earth element content in the bulk sample. Therefore, DaG 489 has the potential of providing us with a further petrogenetic link between the basaltic and lherzolitic shergottites.

Noble gases data show that DaG 489 has an ejection age of ~1.3 Ma. This young age lends support to the requirement of several ejection events to produce the current population of shergottites, nakhlites, and chassignites (SNC) meteorites.

In terms of texture, mineral and bulk compositions, shock level, and weathering features, DaG 489 is essentially identical to DaG 476, another basaltic shergottite independently found ~25 km due north-northeast of DaG 489. Because DaG 489 also has the same exposure history as DaG 476, it is very likely that both meteorites are fragments of the same fall.

In addition to the existing hypotheses on the petrogenesis of the similar EETA79001 lithology A and the identical DaG 476, we propose that DaG 489 could have formed through high-degree partial melting of a lherzolite-like material.

INTRODUCTION

Thirteen meteorites (shergottites, nakhlites, and chassignites; (SNC)) are basaltic and ultramafic igneous rocks that plot on a specific O-isotopic fractionation line (*e.g.*, Franchi *et al.*, 1999) and share geochemical characteristics indicating that they originated from a common mantle source-region of a large planetary body, distinct from those of all other known meteorites (*e.g.*, McSween, 1994). Primarily because of the close match of the shock-implanted gases found in some of these meteorites to the martian atmosphere abundances determined by the Viking landers in 1976, SNC meteorites are believed to have originated from the planet Mars (Bogard and Johnson, 1983; Bogard *et al.*, 1984; Becker and Pepin, 1984, 1986; Swindle *et al.*, 1986; Wiens *et al.*, 1986). As such these are important samples for the opportunity they offer in developing our understanding of the geological evolution of the red planet (McSween, 1994).

By far the most common type of martian meteorites are the shergottites. They can be divided into two subgroups (*e.g.*, McSween, 1994; McSween and Treiman, 1998): lherzolitic shergottites (Allan Hills (ALH) 77005, Lewis Cliff (LEW) 88516, and Yamato (Y)-793605); and basaltic shergottites (Shergotty, Zagami, Queen Alexandra Range (QUE) 94201, Elephant Moraine (EET) A79001, and Dar al Gani (DaG) 476). Lherzolitic shergottites are pyroxene and olivine cumulates formed in plutonic environments. Basaltic shergottites are pyroxene and maskelynite (after plagioclase in response to shock) rocks thought to sample shallow intrusions or lava flows. Meteorite EETA79001 consists of two main lithologies, separated by an igneous contact: lithology A, where a basalt entrains lherzolitic xenocrysts and xenoliths, and lithology B, which is similar to QUE 94201 (Mikouchi *et al.*, 1998). Dar al Gani 476 is similar to the lithology A of EETA79001 (Zipfel *et al.*, 1999, 2000; Mikouchi, 1999). All other martian meteorites (*e.g.*, McSween, 1994; McSween and Treiman, 1998) have cumulate textures and include three clinopyroxenites–wehrlites or nakhlites (Nakhla, Lafayette, and Governador Valadares), one dunite (Chassigny), and one orthopyroxenite (ALH 84001).

A new martian meteorite of 2146 g (Fig. 1) was found in the Dar al Gani region of the Libyan Sahara (~27°08' N, 16°05' E; Fig. 2) by an anonymous meteorite finder, during one of his search campaigns in 1997–98. Late in 1998, the stone was loaned to the Museo Nazionale dell'Antartide of the University of Siena (MNA-SI) for hand-specimen description, and two fragments totalling 34.9 g (specimens DaG 489/A and DaG 489/B; Fig. 1b) were donated to the museum for classification and further research. The meteorite,

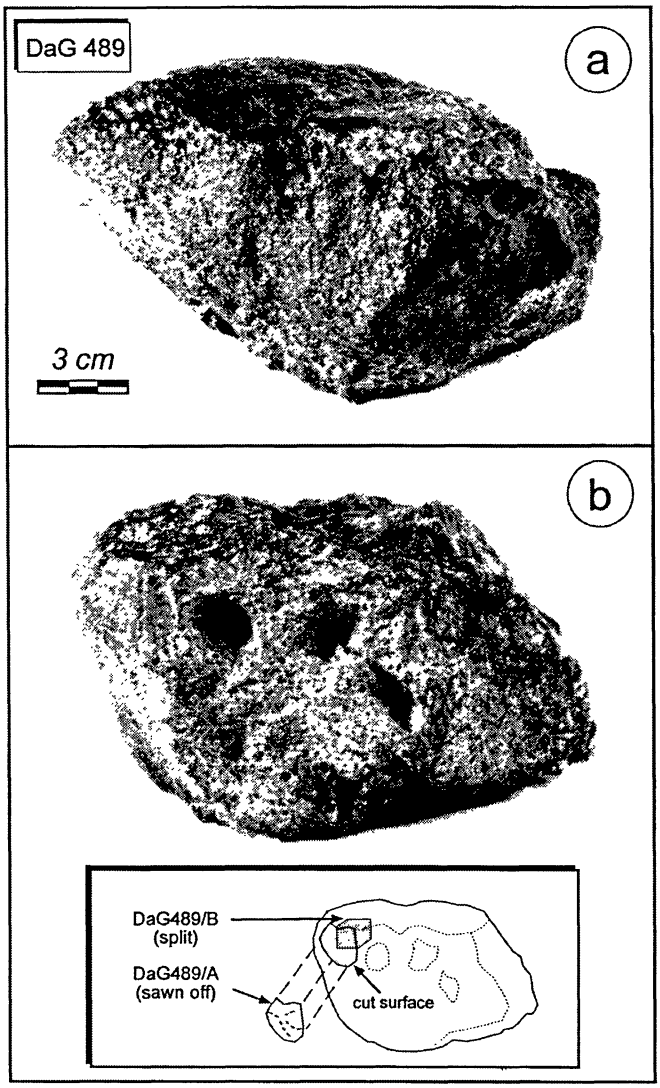

FIG. 1. The 2146 g DaG 489 martian meteorite. (a) Dar al Gani 489 is devoid of fusion crust, but it is coated by a dark brown film of desert varnish. The speckled appearance, emphasized by side illumination, is due to the occurrence of millimeter-sized phenocrysts of olivine. (b) The pale brown surface in the foreground was once buried in the sand and shows the porphyritic texture. The three centimeter-sized hollows are remnants of regmaglypts or possibly wind-carved sculptures. (Inset) Dar al Gani 489/A and /B are the two specimens donated to the MNA-SI by the finder for research. Thin sections and aliquots used for this study were taken from DaG 489/A.

named Dar al Gani 489 (DaG 489), turned out to be a basaltic shergottite, as recently announced by some of us in the Meteoritical Bulletin No. 83 (Grossman, 1999). Dar al Gani 489 is thus the second martian basalt from Dar al Gani after DaG 476 (Grossman, 1999; Zipfel *et al.*, 2000), a 2015 g stone independently found in 1998 ~25 km due north-northeast of DaG 489 (Fig. 2).

In this paper, we expand on the first announcement of DaG 489 (Grossman, 1999; Folco *et al.*, 1999) to report on petrography and mineralogy, bulk chemistry, O-isotopic and noble gas data, and to discuss petrology and possible pairing with DaG 476.

HAND SPECIMEN DESCRIPTION

Dar al Gani 489 is an approximately 16 × 9 × 10 cm angular meteorite fragment (Fig. 1), it weighs 2146 g, and it is devoid of

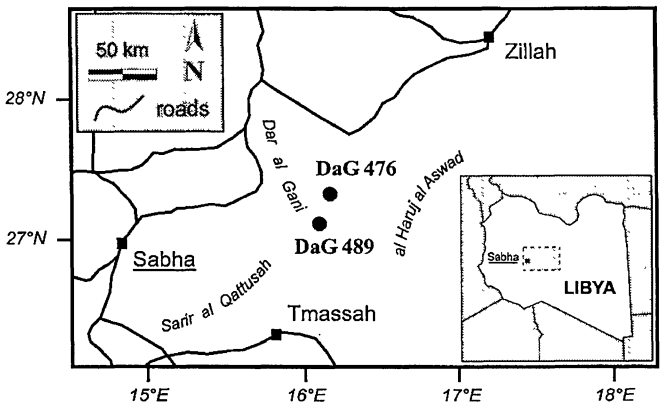

FIG. 2. Sketch map of the Dar al Gani region showing find locations of DaG 489 and DaG 476. Geographic coordinates for DaG 476 are from Grossman (1999).

fusion crust. The external surface is partially coated by a dark-brown film of desert varnish (Fig. 1a) and flecked with millimeter-sized dark phenocrysts (olivine) in relief; only the surface that had been buried in the sand (Fig. 1b) appears pale-brown and bears three characteristic centimeter-deep hollows, possibly remnants of regmaglypts or wind-carved reliefs. On freshly cut surfaces, the phenocrysts appear black coloured and set in a dark-green groundmass. The lithology of the meteorite appears to be homogeneous and isotropic.

Fracturing is moderate and not pervasive; some fractures are filled in by carbonate deposits (calcite) or loose soil. Carbonate deposits are relatively abundant in the outer, ~3 mm deep, shell of the sample, but significantly decrease towards the interior. Indeed, the mechanical splitting of specimen DaG 489/B (Fig. 1b) from the interior of the sample was much more characteristic of a fresh achondrite.

PETROGRAPHY AND MINERALOGY

Two polished thin sections from different areas of the DaG 489/A specimen (DaG 489A,01 and ,03) and totalling 130 mm^2 were prepared for petrographic investigation under optical microscope and microanalytical scanning electron microscope (SEM) Philips XL30. Mineral mode was determined through counting of 8162 points (spacing 70 μm) in the thin sections under the SEM. Mineral compositions were obtained by means of electron microprobe (EMP) JEOL JXA 8600, fitted with four wavelength dispersive spectrometers. Running conditions were 15 kV accelerating voltage and 10 nA beam current on a Faraday cage. Counting time was 15 s at both peak and background for Si and Mg, 10 s for Na and 40 s for all other elements. Nominal beam spot was 1 μm for the analyses of all minerals but feldspathic glass and merrillite, for which a defocussed beam, from 5 to 15 μm according to grain-size, was employed to reduce the undesirable migration of volatile elements. The method by Bence and Albee (1968) was employed for data reduction. A number of synthetic and mineral standards were used for instrumental calibration.

In thin section, DaG 489 exhibits a porphyritic texture, given by medium-grained, olivine crystals (typically from 0.5 up to 2 mm in apparent diameter) set in a fine-grained groundmass (average grain size 0.1 mm), consisting of pigeonite crystals and interstitial feldspathic glass (Fig. 3a–c). Olivine crystals sometime occur in clusters of two or three individuals (Fig. 3a). Some elongated olivine crystals and lath-shaped pyroxenes are slightly oriented (Fig. 3b),

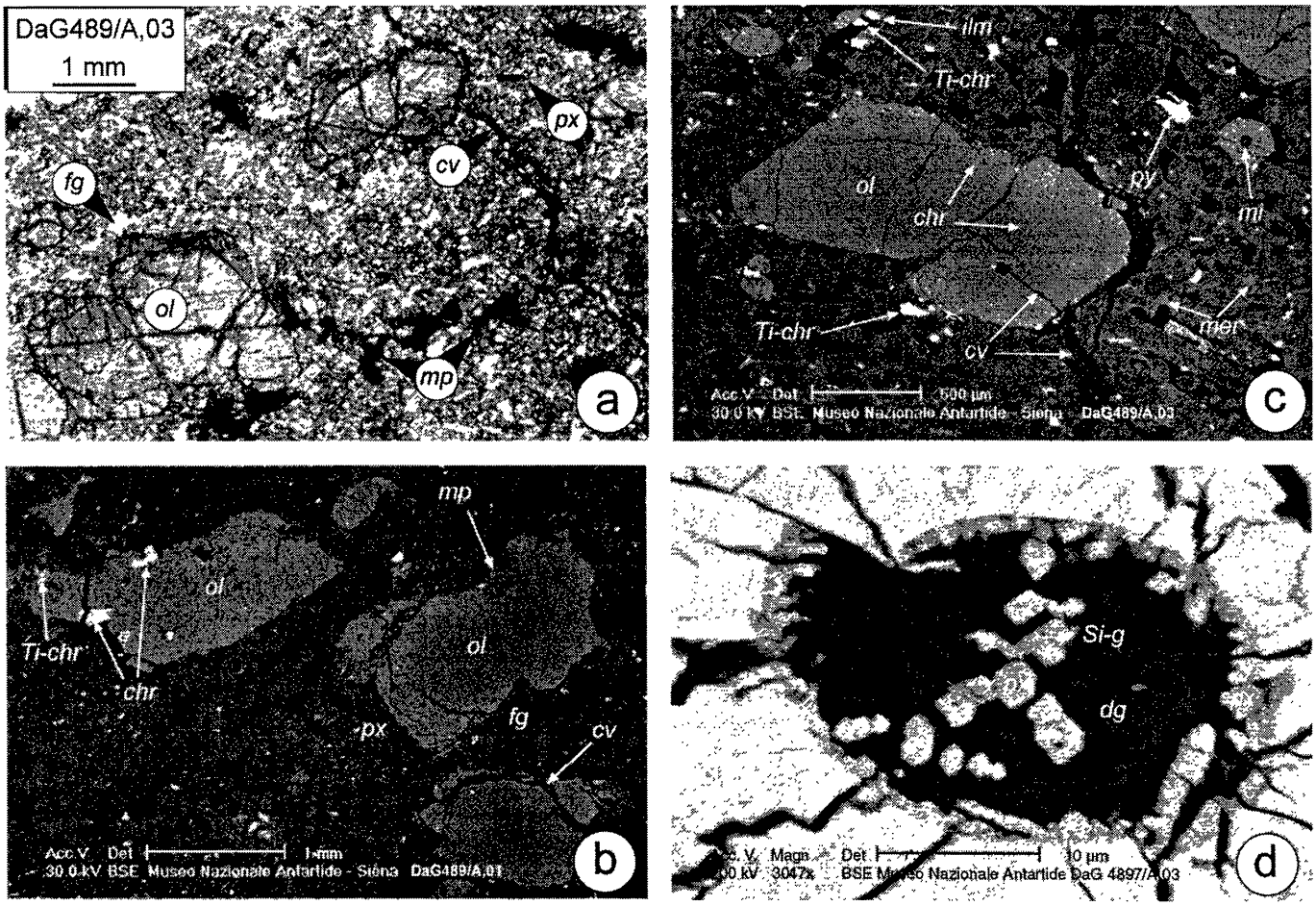

FIG. 3. Photomicrographs from DaG 489 thin sections DaG 489/A,01 and ,03. (a) Millimeter-sized olivine crystals set in a fine-grained matrix consisting of lath-shaped pyroxene and colourless, interstitial feldspathic glass (transmitted light). (b) Zoning and corrosion microstructures in olivine crystals; some olivine grains are locally aligned outlining a not pervasive magmatic foliation (backscattered electron image); the large olivine crystal on the top left shows virtually no compositional zoning Fo_{63-60} and several "apparent inclusions" of groundmass material (*i.e.*, pigeonite and large chromite) as an effect of the thin section plane, which cuts across the interface between a corroded olivine rim and the groundmass. (c) Olivine and trapped magmatic inclusions (backscattered electron image). (d) Close-up of a magmatic inclusions (overexposed backscattered electron image); the needle-shaped pyroxenes free-floating in the glassy matrix are here cut close to their basal plane. Abbreviations: ol = olivine, px = pyroxene, fg = feldspathic glass, chr = chromite, Ti-chr = Ti-chromite, ilm = ilmenite, py = pyrrhotite, mr = merrillite, mp = impact-melt pocket, cv = carbonate vein, mi = magmatic inclusion, dg = dacitic glass, Si-g = Si-rich glass.

outlining a weak magmatic foliation: this foliation is not penetrative, because it is not recognised at the scale of the hand-specimen. Minor mineral components include enstatite, augite, chromite, Ti-chromite, ilmenite, merrillite, pyrrhotite, secondary calcite, and iron oxides. Mineral mode is 20% olivine, 54% pyroxene (50% pigeonite, 4% enstatite, traces of augite), 17% feldspathic glass, 3% spinels and iron sulphide, 1% merrillite, 4% melt pockets, 1% calcite, and traces of iron oxides (Table 1). Fracturing, planar deformation features, and strong mosaicism in olivine, fracturing, and undulose extinction in pyroxene, along with abundant shock-induced melt pockets and veinlets (Fig. 3a–c) indicate major shock metamorphism (*i.e.*, shock stage S5 or higher after the classification scheme by Stöffler *et al.*, 1991). Calcite veins, usually tens of micrometers thick, run along and across grain boundaries and shock veins (Fig. 3a–c). They are weathering products that likely formed on the caliche-rich soils of the Dar al Gani desert.

Olivine crystals display a distinctive yellow to brown colour in transmitted light and a characteristic speckled appearance because of an even distribution of tens of opaque, micrometer-sized inclusions (chromite) in each crystal. Olivines show corrosion microstructures (Fig. 3b): magnesian cores with subhedral outlines are overgrown

TABLE 1. Modal composition of DaG 489 obtained by point counting on DaG 489/A,01 and ,03 thin sections.*

Meteorite	DaG 489	DaG 476	
Source	This work (vol%)	Zipfel *et al.* (2000) (vol%)	Mikouchi (1999) (vol%)
pyroxene	54	58–60	59
-pigeonite	50	52	–
-augite	tr	2.8	–
-enstatite	4	1.5–3.4	–
olivine	20	14–17	24
feldspathic glass	17	14–17	12
merrillite	1	tr	1
opaques	3†	2.6–3.8†	2‡
impact-melt pockets	4	4.0–4.5	–
calcite	1	2.2–2.7	2

*Data from DaG 476 are reported for comparison.
tr = traces.
†Includes chromite and Ti-chromites, ilmenite, and Fe-sulfides.
‡Includes ilmenite and Fe-sulfides.

by irregularly developed Fe-rich rims, with jagged and embayed contours pervaded by groundmass material. Compositions from core to rim span from Fo_{79} to Fo_{59} (Fig. 4 and Table 2). The larger grains usually have the most magnesian core compositions. The extent of the compositional zoning may largely vary from crystal to crystal but appear to decrease with apparent grain size, as a possible effect of off-centre grain cut on the thin section plane. Olivines also show a rather high Ca content (CaO = 0.25 average wt%). Magmatic inclusions (see below) occur at the cores of some crystals.

Pigeonite crystals are pale-brown in transmitted light, optically striated parallel to (100) in crossed polars (possibly shock twinning) and show euhedral to subhedral lath-like shapes (Fig. 3b,c). They are zoned with Fe- and Ca-poor cores and discontinuous Fe- and Ca-rich rims, within the En_{75} Wo_5 to En_{57} Wo_{15} range (Fig. 4, Table 2). Low-Ca pyroxene with enstatitic composition, ranging from En_{82} Wo_2 to En_{71} Wo_4, occurs at the cores of some pigeonite crystals in the form of square-shaped zones up to some tens of micrometers across (Fig. 4, Table 2). This low-Ca pyroxene is here referred to as enstatite on a compositional basis (*i.e.*, according to Morimoto, 1988), because its dominant constituent polymorph is yet to be determined. In both enstatite and pigeonite, TiO_2, Cr_2O_3, and Al_2O_3 range from 0.04 to 0.30, from 0.30 to 0.65, and from 0.60 to 1.3 wt%, respectively. Augite occurs as inclusions up to few tens of micrometers in size in enstatite, olivine, and large chromites. Augite composition is relatively uniform in individual grains, but different grains show a small compositional variation in the En_{48-52} Wo_{29-32} range (Fig. 4, Table 2).

The gaps between olivine, pyroxene, chromite, and pyrrhotite grains are filled in by interstitial, clear and colourless glass with variable labradoritic composition, within the An_{67-56} Or_{0-1} range (Figs. 3 and 4; Table 2). Significant compositional variations are observed from glass patch to patch, whereas individual glass patches show a subtle compositional zoning with Na increasing and Ca decreasing towards the periphery. Potassium is present in minor amounts (K_2O < 0.10 wt%) and appears correlated with Na. Glass also contains relatively high amounts of Fe and Mg (FeO = 0.37 and MgO = 0.22 average wt%). The evidence for shock stage ≥S5 outlined above and the stoichiometric feldspathic composition of the glass suggest that the glass formed by amorphization of plagioclase (maskelynite) in response to major shock.

Pyrrhotite up to 100 μm in size was primarily found in the matrix in the form of blocky crystals with lobate or fringed contours set in the feldspathic glass (Fig. 3b,c). It has a Fe/S atomic ratio of 0.9 and contains minor amounts of Ni and Co (Table 2). In addition, euhedral, micrometer-sized crystals are occasionally associated with pigeonite inclusions in the olivine phenocrysts. Chromite (Fig. 3b,c) occurs in the groundmass as subhedral crystals up to 200 μm in size with rounded outlines and as micrometer-sized subhedral crystals in olivine (speckled appearance of olivine) with indistinguishable composition. Titanian chromite was found either as discrete crystals merged in the groundmass, or as rims, up to some tens of micrometers wide, around the larger chromite grains. The Ti-chromite is often zoned with ulvöspinel mole fraction increasing towards the periphery, and intergrown with ilmenite, sometimes in the form of exsolved lamellae up to some micrometers thick. Magmatic inclusions were found in one large chromite crystal (see below). Merrillite, up to some tens of micrometers across, was found as intergranular anhedral grains between adjacent pigeonite crystals. It is essentially a calcium-phosphate with some substitution of Mg, Na, and Fe for Ca, and chemical formula close to $Ca_{8.64}(Mg,Fe)_{1.08}Na_{0.54}(PO_4)_7$.

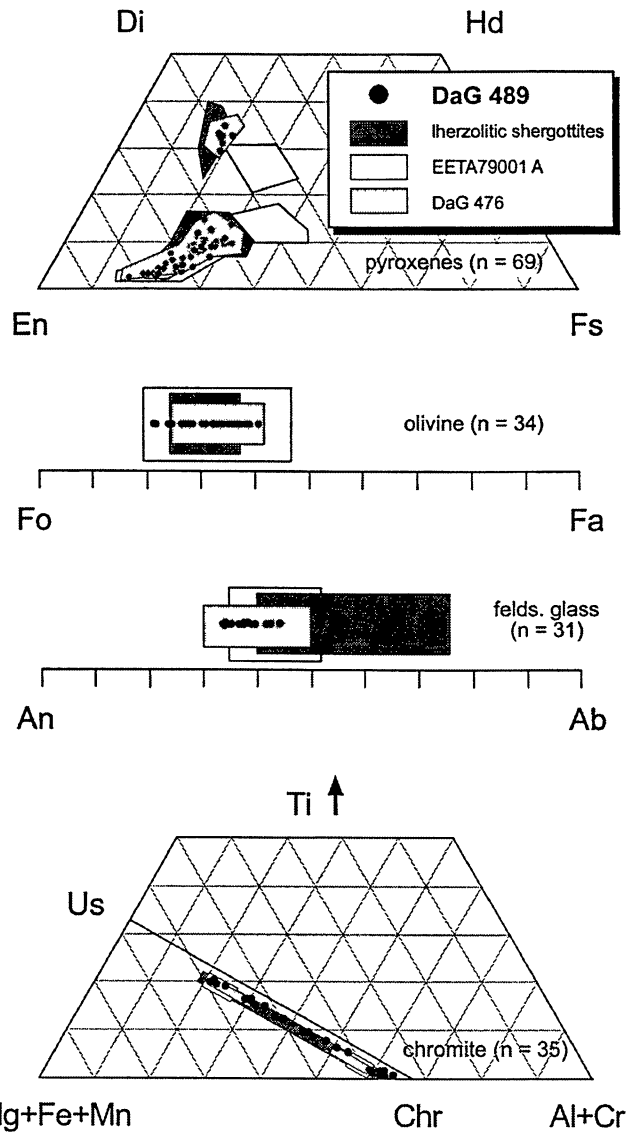

FIG. 4. Mineral compositions of DaG 489 pyroxenes, olivine, feldspathic glass, and chromite. Data from DaG 476 (Zipfel *et al.*, 2000), EETA79001 lithology A (Steele and Smith, 1982; McSween and Jarosewich, 1983), lherzolitic shergottites Y-793605 (Ikeda, 1997; Mikouchi and Miyamoto, 1997), ALH 77005 (McSween *et al.*, 1979; Ikeda, 1994), and LEW 88516 (Harvey *et al.*, 1993) are shown for comparison.

Both Cl and F contents were below detection limit. Merrillite, chromite, Ti-chromites, and ilmenite are all characterised by high Mg contents (MgO, approximately 3 to 5 wt%; Table 2).

A few magmatic inclusions were found trapped near the centres of some olivine crystals (Fig. 3c,d) and in one large chromite grain. They show rounded shapes and range in size from a few tens to some tens of micrometers in diameter. Cracks radiate out from the inclusions into the host crystals. The inclusions principally consist of micrometer-sized crystallites of aluminous Ca-rich pyroxenes set in a glassy matrix. The pyroxenes grow at the inclusion walls or occur as needle-shaped crystals free-floating in the glassy matrix. The matrix consists of two compositionally different glasses showing a liquid immiscibility fabric: blebs of silica-rich glass containing up to ~80 wt% SiO_2 (Table 3) are set in a moderately silica-rich glass with approximate dacitic composition ($SiO_2 \approx 63$ wt%,

TABLE 2. Representative EMP analyses of major phases of DaG 489.

	Olivine		Enstatite	Pigeonite		Augite	Felds. glass		Merrillite	Chromite		Ilmenite	Pyrrhotite	
	core	rim		core	rim		An-rich	An-poor		high-Ti				
Oxides wt%													**At%**	
SiO_2	38.51	36.71	56.10	55.08	52.71	51.99	51.38	53.53	0.22	–	–	–	S	52.7
TiO_2	–	–	0.04	0.06	0.16	0.32	–	0.08	–	1.20	23.05	53.49	Fe	46.9
Al_2O_3	–	–	0.81	0.78	1.03	1.76	30.82	29.18	–	8.46	4.05	0.09	Co	0.0
Cr_2O_3	–	–	0.52	0.44	0.52	1.38	–	–	–	56.32	16.55	0.31	Ni	0.2
Fe_2O_3*	–	–	–	–	–	–	–	–	–	2.43	4.86	0.84	sum	99.9
FeO	22.78	32.81	12.27	15.07	18.40	11.40	0.40	0.34	1.38	26.79	47.71	40.93		
MnO	0.48	0.76	0.37	0.57	0.56	0.43	–	–	0.05	0.59	0.69	0.68		
MgO	38.59	30.07	29.30	25.93	21.87	17.23	0.16	0.22	3.45	4.76	3.39	3.59		
CaO	0.17	0.21	1.15	2.79	5.18	15.58	13.62	11.60	46.87	0.06	–	0.17		
Na_2O	nd	nd	–	–	–	0.28	3.65	4.79	1.63	–	–	–		
K_2O	nd	nd	–	–	–	–	0.03	0.09	–	–	–	–		
P_2O_5	nd	nd	nd	nd	nd	nd	nd	nd	46.51	nd	nd	nd		
Sum	100.53	100.56	100.52	100.71	100.43	100.36	100.06	99.83	100.10	100.60	100.31	100.10		
a.p.f.u. on:	4 O		6 O	6 O		6 O	8 O		27 O	24 cat		2 cat		
Si	0.999	1.001	1.986	1.983	1.944	1.922	2.336	2.426	0.038	–	–	–		
Al	–	–	0.034	0.033	0.045	0.077	1.650	1.557	–	2.744	1.359	0.003		
Ti	–	–	0.001	0.002	0.004	0.009	–	0.003	–	0.248	4.937	0.988		
Cr	0.001	0.001	0.015	0.013	0.015	0.040	–	–	–	12.256	3.727	0.006		
Fe^{3+}*	–	–	–	–	–	–	–	–	–	0.503	1.041	0.016		
Fe^{2+}	0.494	0.748	0.363	0.455	0.567	0.352	0.015	0.013	0.198	6.165	11.362	0.840		
Mn	0.011	0.018	0.011	0.016	0.017	0.013	–	–	0.007	0.112	0.136	0.012		
Mg	1.492	1.223	1.546	1.391	1.202	0.949	0.011	0.015	0.885	1.953	1.439	0.131		
Ca	0.005	0.006	0.044	0.107	0.205	0.617	0.663	0.563	8.635	0.018	–	0.004		
Na	–	–	–	–	–	0.020	0.322	0.421	0.543	–	–	–		
K	–	–	–	–	–	–	0.002	0.005	–	–	–	–		
P	–	–	–	–	–	–	–	–	6.771	–	–	–		
Sum	3.001	2.999	4.000	4.000	3.999	3.999	4.999	5.003	17.078	–	–	–		
Fo/En/Or	75.1	62.0	78.7	70.7	60.4	49.1	0.2	0.5	–	–	–	–		
Wo/An	–	–	2.2	5.5	10.3	32.0	67.2	56.9	–	–	–	–		

*Fe_2O_3 and Fe^{3+} from stoichiometric criteria; nd = not determined.

TABLE 3. Electron microprobe analyses of glass and pyroxene of melt inclusions in DaG 489 olivines.

	Dacitic glass	Si-rich glass	Pyroxene
Oxides wt%			
SiO_2	63.15	80.49	46.91
TiO_2	0.28	0.21	2.57
Al_2O_3	21.62	10.71	9.45
Cr_2O_3	–	–	0.20
FeO	3.23	1.48	9.62
MnO	–	–	0.30
MgO	0.6	0.27	9.21
CaO	5.40	2.56	21.54
Na_2O	3.52	1.85	0.43
K_2O	0.43	0.39	–
Sum	98.22	97.96	100.23

$Na_2O + K_2O \approx 4$ wt%). Occasional tiny grains of iron sulphides and ilmenite were observed in one inclusion.

Shock-induced melt pockets and microveins (Fig. 3a,b) mainly consist of glass with feldspathic composition (An_{56} Or_1), and relic crystals of olivine and pyroxene with resorbed outlines. Glass is turbid brown in transmitted light and bears swarms of crypto-crystalline, Fe-Mg bearing mineral inclusions. Some later offset is observed in some veins.

Texture, mineral abundances, and compositions of DaG 489 are those of an olivine-basalt (Le Maitre, 1989). The assemblage of relatively ferroan mafic minerals and labradoritic composition of feldspathic glass (after plagioclase) are consistent with a martian origin and not lunar, terrestrial, or eucritic (*e.g.*, McSween *et al.*, 1979). Likewise, distinctive markers of planetary environments (*e.g.*, Papike, 1998) including the K atoms-per-formula-unit (a.p.f.u.) *vs.* An content in plagioclase and the Fe/Mn atomic ratio in olivine and pyroxene indicate that DaG 489 is martian (Fig. 5): the feldspathic glass composition of DaG 489, with Fe < 0.016 a.p.f.u., K < 0.09 a.p.f.u., and percent of An ranging from 56 to 67, fall in the SNC range, and it is distinct from plagioclases of lunar, terrestrial, and eucritic basaltic rocks; the $Fe/Mn_{(a.p.f.u.)}$ in olivine (from 40 to 50) and pyroxene (from 29 to 40 in pigeonite, from 30 to 43 in enstatite, and from 25 to 32 in augite) is consistent with martian or eucritic meteorites, and not with lunar or terrestrial basaltic rocks. According to McSween (1994) and McSween and Treiman (1998), DaG 489 can be classified as a highly shocked (≥S5), basaltic shergottite.

However, the mineralogical assemblage of DaG 489 (Table 1, 2, and Fig. 4) closely matches that of lherzolitic shergottites Y-793605 (Ikeda, 1997; Mikouchi and Miyamoto, 1997), ALH 77005 (McSween *et al.* 1979; Ikeda, 1994), and LEW 88516 (Harvey *et al.*, 1993), and not that of the typical basaltic shergottites Shergotty, Zagami, QUE 94201, and lithology B of EETA79001 (*e.g.*, Stolper and McSween, 1979; McSween and Jarosewich, 1983; Mikouchi *et al.*, 1998; McSween and Treiman, 1998). Basaltic shergottites lack enstatitic pyroxene and contain only traces of fayalitic olivine and magnesian chromite and bear magnesium-poorer pigeonite, augite, merrillite, and ilmenite. On the other hand, the compositional range of the feldspathic glass in DaG 489 is close to basaltic shergottites QUE 94201 and EETA79001 lithology B and overlap the An-rich trend observed in Zagami, Shergotty, and lherzolitic shergottites.

The large olivine and chromite crystals of DaG 489 have rounded shapes and corrosion microstructures because of disequilibrium interaction with the surrounding basaltic melt and closely resemble those found in lherzolitic shergottites: the size, core compositions,

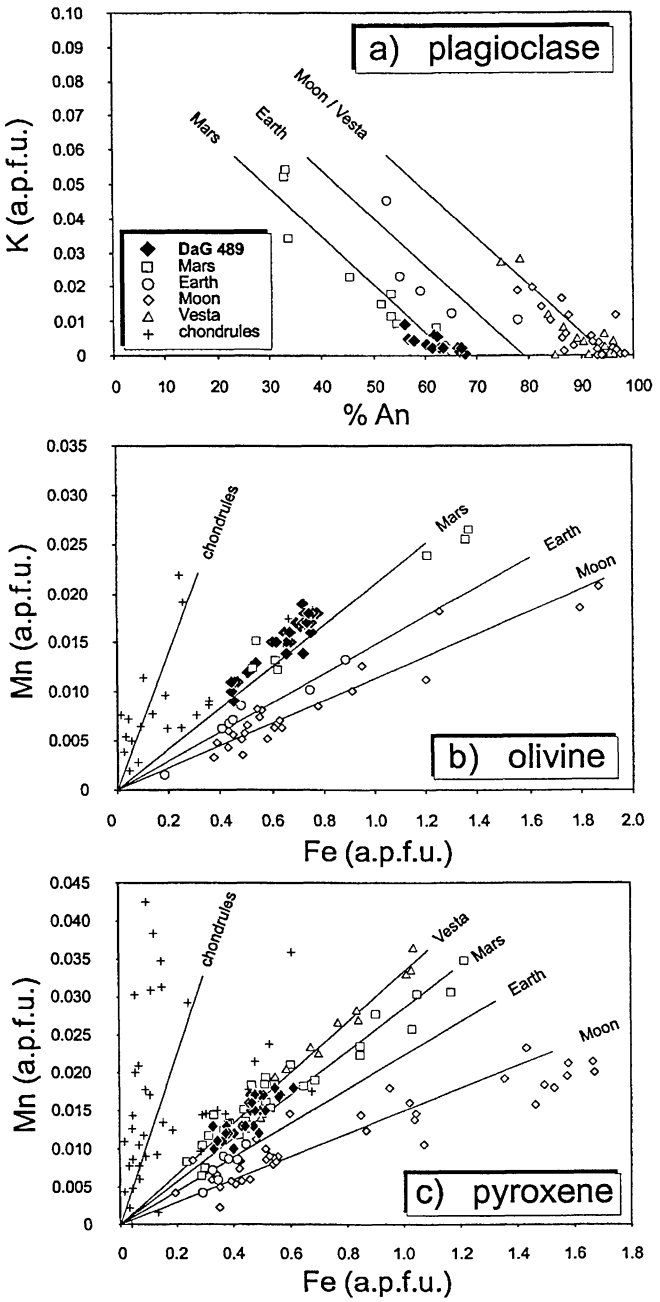

FIG. 5. Potassium *vs.* percent of anorthite in plagioclase (a), Mn *vs.* Fe (a.p.f.u.) in olivine (b) and pyroxene (c) for DaG 489 and for planetary igneous rocks (modified after Papike, 1998). Trend lines are approximate.

abundance, and type of inclusions (in particular the magmatic inclusions) of olivines, and the size and chemical composition of chromites of DaG 489 are essentially indistinguishable from those of the large olivine and chromite crystals occurring in Y-793605 (Ikeda, 1997; Mikouchi and Miyamoto, 1997), ALH 77005 (McSween *et al.*, 1979; Ikeda, 1994), and LEW 88516 (Harvey *et al.*, 1993).

Dar al Gani 489 is therefore similar to the hybrid shergottite lithology A of EETA79001 (*e.g.*, Steele and Smith, 1982; McSween and Jarosewich, 1983) in terms of texture, mineral composition, corrosion microstructures in olivine, and shock level. However, some differences do exist. For instance, in contrast to EETA79001

lithology A, DaG 489 does not bear millimeter-sized megacrysts of pyroxene with enstatitic composition and contains more olivine (in EETA79001 lithology A modal olivine is 7–13 vol%; Steele and Smith, 1982; McSween and Jarosewich, 1983). Furthermore, olivine, pigeonite, and feldspathic glass compositions of DaG 489 do not extend to the Fa-rich, Fs-rich, and Ab-rich trend observed in EETA79001 lithology A, and augite composition is distinctly Ca- and Mg-richer (Fig. 4).

On the basis of the petrographic description above, we observe that DaG 489 is essentially identical to DaG 476 (Zipfel *et al.*, 2000; Mikouchi, 1999): texture, mineral abundances and compositions, microstructures, shock level, and weathering features are indistinguishable (see also Table 1 and Fig. 4). In addition to that observed for DaG 476 by Zipfel *et al.* (2000) and Mikouchi, (1999), we report the occurrence of exsolved ilmenite in Ti-chromite and a compositional variation of Ti-chromite as large as in lherzolitic shergottites for DaG 489.

BULK CHEMISTRY

A 1.5 g fragment, taken from the interior portion of specimen DaG 489/A, was finely grounded in a virgin agate bell-jar for bulk chemical analyses (Table 4). An aliquot of 750 mg was ignited at 1000 °C (microwave muffle CEM 300) to determine the loss on ignition (LOI) and then fluxed with an excess of $Li_2B_4O_7$ (1:7 weight ratio) for SiO_2, TiO_2, Al_2O_3, Fe_2O_3, MgO, CaO, and P_2O_5 determination by x-ray fluoresence (XRF) (Philips PW 1480). Determination of Na_2O and K_2O was done by atomic absorption spectroscopy (AAS) (Philips PU 9200) on a 200 mg aliquot. The concentration of an additional 39 elements was determined by inductively-coupled plasma mass spectrometry (ICP-MS) (Fisons PQII + STE). An aliquot of 70 mg was dissolved in a PFA vessel on a hot plate at 120 °C, by using HF + HNO_3 purified by subboiling distillation (D'Orazio and Tonarini, 1997). The sample solution, at ~1:1,000 dilution, was measured in replicates by external calibration. Analytical results and precision, along with detection limits, are reported in Table 4.

The bulk composition of DaG 489 confirms that it is a martian meteorite belonging to the shergottite group: key element ratios, such as Fe/Mn = 42.1, Al/Ti = 10.6, Na/Ti = 1.9, P/Ti = 1.0, Ni/Co = 4.3, Ni/Mg = 0.002, and $Co_{(ppm)}/(MgO + FeO)_{(wt\%)}$ = 1.4 (*e.g.*, McSween *et al.*, 1979; Treiman *et al.*, 1986) fall in the typical ranges of SNC meteorites and, in particular, elemental abundances closely match those of shergottites.

The relatively high LOI value (2.25 wt%), coupled with the anomalously high contents of Cs, Ba, U, Ca, and Sr, can be related to the occurrence of calcite microveins and possibly of hydrous phases (see next section) formed during weathering in the Dar al Gani area. Likewise, the anomalously high K/La ratio (1712), a further diagnostic element ratio for SNC meteorites, could be due to selective enrichment of K during hot desert weathering (Bischoff *et al.*, 1998). A similar weathering pattern was observed for DaG 476 by Zipfel *et al.* (2000).

Although DaG 489 is characterised by texture and modal composition similar to basaltic shergottites, it shows bulk chemistry closer to lherzolitic shergottites. This is particularly evident on considering its high $Mg/(Mg + Fe)_{(molar)}$ = 0.68; its high content of Cr, Co, Ni, and its low content of Na, Al, Sc, Ti, V; and light rare earth elements (LREE), which reflect the high abundance of modal olivine, pyroxene with enstatitic composition, and chromite. Dar al Gani 489 shows a LREE-depleted chondrite-normalized pattern (Fig. 6) with La_N = 0.66 and Yb_N = 4.9. Light rare earth elements are highly fractionated ($[La/Nd]_N$ = 0.54) and are characterised by unusual $[La/Ce]_N$ and $[Pr/Nd]_N$ very close to 1. The step-like normalised distribution of LREE hinders the detection of possible anomalies. The medium rare earth element (MREE) segment of the

TABLE 4. Bulk chemistry of DaG 489.

	DaG 489 (average of two replicates)	Detection limit (ppm)	Precision (RSD%)
SiO_2 (wt %)	47.72	–	–
TiO_2	0.35	–	–
Al_2O_3	4.19	–	–
Fe_2O_3	18.36	–	–
MnO	0.394	–	–
MgO	19.36	–	–
CaO*	7.83	–	–
Na_2O	0.550	–	–
K_2O*	0.033	–	–
P_2O_5	0.49	–	–
LOI	2.25	–	–
Li (ppm)	2.60	0.002	3
Be	<0.04	0.04	–
Sc	28	0.03	3
V	171	0.02	3
Cr	4603	0.3	3
Co	50	0.003	3
Ni	214	0.05	3
Cu	6.7	0.1	7
Zn	49	0.3	5
Rb	0.89	0.03	10
Sr*	87	0.03	3
Y	8.2	0.007	3
Zr	8.1	0.03	5
Nb	0.13	0.001	5
Mo	0.18	0.1	>10
Cs*	0.56	0.002	5
Ba*	48	0.07	3
La	0.16	0.004	10
Ce	0.40	0.005	7
Pr	0.11	0.004	10
Nd	0.56	0.01	7
Sm	0.38	0.008	10
Eu	0.22	0.004	7
Gd	1.00	0.01	5
Tb	0.20	0.002	5
Dy	1.38	0.002	3
Ho	0.30	0.002	5
Er	0.87	0.02	10
Tm	0.13	0.004	10
Yb	0.79	0.01	7
Lu	0.12	0.003	10
Hf	0.36	0.003	5
Ta	0.01	0.002	>10
W	0.24	0.04	>10
Tl	0.02	0.004	>10
Pb	<0.04	0.04	–
Th	0.02	0.005	>10
U*	0.14	0.004	10

Detection limits (ppm in the solid sample) are estimated by calculating the concentration corresponding to three times the standard deviation of the blank solution counts and assuming a 1:1000 sample dilution. Precision is based on repeated analyses of geochemical reference materials with composition comparable to that of DaG 489.
*Elements with concentrations possibly altered by terrestrial weathering.
LOI = loss on ignition.

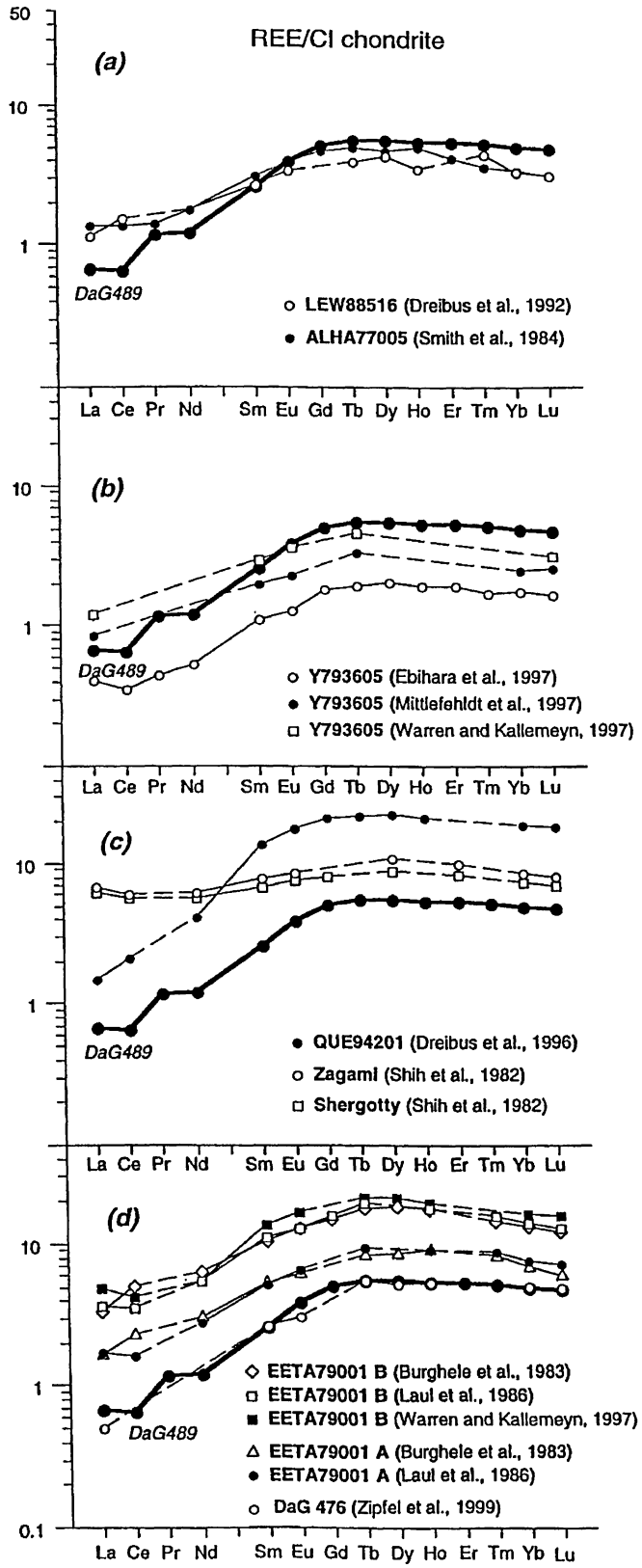

FIG. 6. The CI chondrite-normalized bulk-rock REE patterns for DaG 489, other lherzolitic (a, b) and basaltic (c, d) shergottites. Normalizing values after McDonough and Sun (1995).

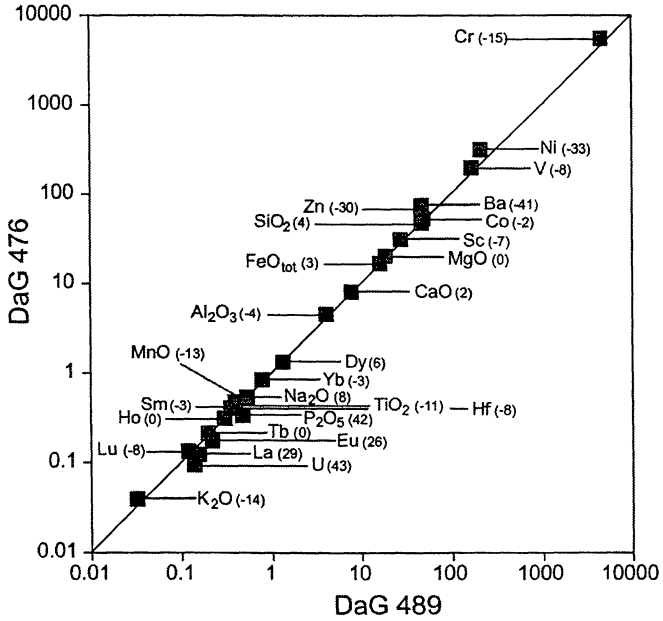

FIG. 7. Comparison between bulk chemical compositions of DaG 489 and DaG 476. Elements Si, Ti, Al, Fe, Mn, Mg, Ca, Na, K, and P are given as wt% of the oxide; all other elements are given in ppm. Numbers in parentheses are the percent difference for each element given by $(X_{DaG489}-X_{DaG476})/X_{mean} \times 100$. Data for DaG 476 are from Zipfel *et al.* (2000), Table 3, columns 2–3.

pattern displays a smooth upward-convex curvature without any significant Eu-anomaly, whereas the heavy rare earth element (HREE) segment is gently inclined toward Lu ($[Ho/Lu]_N = 1.14$). The LREE-depleted pattern along with the MREE upward-convex pattern is a common feature to all known lherzolitic shergottites (Fig. 6a,b) and is also observed, although at higher concentrations, in the basaltic shergottite QUE 94201 and EETA79001 lithology B, and in the hybrid shergottite EETA79001 lithology A (Fig. 6c,d). This is consistent with the hybrid petrography of DaG 489 already pointed out in the previous section and explains the almost ultramafic character of DaG 489 (*i.e.*, MgO = 19.36, Fe_2O_3 = 18.36, TiO_2 = 0.35, and $Na_2O + K_2O$ = 0.583; Table 4).

Both major and trace element compositions of DaG 489 and DaG 476 (Zipfel *et al.*, 2000) are remarkably similar: the concentrations of 20 out of 27 elements in the two samples differ by <15% (from a mean of the two samples), with 12 differing by <7% (Figs. 6d and 7).

OXYGEN ISOTOPES

The O-isotopic composition of DaG 489 was determined by laser fluorination (Miller *et al.*, 1999) on ~1 mg aliquots of a 36 mg chip from specimen DaG 489/A (Fig. 1b), crushed in an agate mortar and pestle.

The $\delta^{18}O$ value and corresponding $\Delta^{17}O$ value (Table 5, Fig. 8) clearly show that DaG 489 is indeed a member of the SNC clan, falling within the limited range of $\delta^{18}O$ values of the SNC meteorites and exactly along the martian mass fractionation line defined by Franchi *et al.* (1999).

Although DaG 489 and DaG 476 appear to be petrographically and geochemically (see above) identical, it is noteworthy that the $\delta^{18}O$ value of DaG 489 is distinct from that of DaG 476, being ~0.4‰ heavier. This may be a reflection of sample heterogeneity (*i.e.*, different mineral abundances in the two subsamples). However, a more likely explanation is that it is a reflection of variable levels or

TABLE 5. Oxygen-isotopic composition of DaG 489, DaG 476, and other SNC meteorites.

	$\delta^{17}O$	$\delta^{18}O$	$\Delta^{17}O$
DaG 489	2.89	4.98	0.305
DaG 476*	2.69	4.57	0.316
Other SNC meteorites (n = 10)*	–	–	0.321 ± 0.013

*Data from Franchi *et al.* (1999).

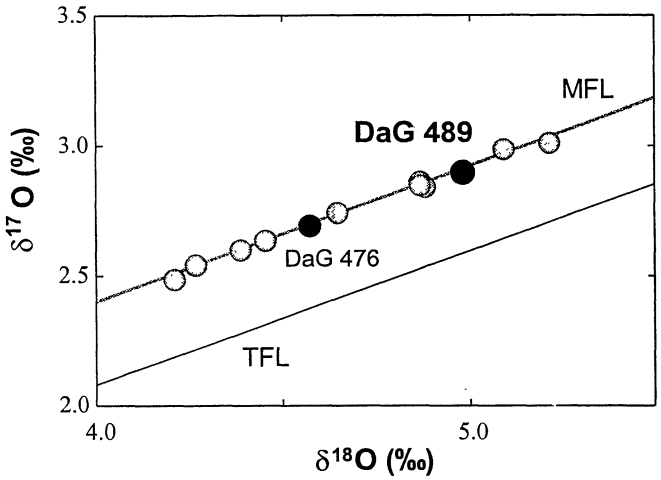

FIG. 8. Oxygen-isotopic composition of DaG 489, DaG 476, and the other SNC meteorites. For reference, the terrestrial fractionation line (TFL) and the martian fractionation line (MFL) are shown. The MFL is a best-fit line through the SNC data and has a slope 0.52, parallel to the TFL. Data for DaG 476 and the other SNCs are from Franchi *et al.* (1999).

types of weathering suffered by the two samples. Although the thorough prefluorination of samples during laser fluorination results in the removal of small amounts of low-temperature weathering products present in most samples, the relatively high degree of weathering in the Dar al Gani SNC meteorites means that some weathering products persist through to the analysis stage. The heterogeneous nature of the weathering in these meteorites means that variations should exist at the level of the small samples used for O-isotopic analysis. That the $\Delta^{17}O$ value of DaG 489 is slightly lower than that of DaG 476, albeit not outside the limits of the technique, does suggest that the higher $\delta^{18}O$ value of DaG 489 may be due to an admixture of a small amount of terrestrial O with a high (approximately +20‰) $\delta^{18}O$ value. Given the parallel relationship between the O-isotopic composition of clay minerals and the meteoritic water line (Hoefs, 1997), such elevated $\delta^{18}O$ values are typical of those expected for clay minerals formed in hot desert environments. Together with calcite, the suspected presence of secondary clay minerals would explain, at least in part, the high LOI value (Table 4) described in the previous section. Clay minerals were not recognised on this scale with the optical and electron microscopes; however, they might be the unresolved Fe-Mg inclusions found in the glass of the shock melt pockets.

NOBLE GASES

The abundance and isotopic composition of He, Ne, Ar, as well as the concentrations of ^{84}Kr, ^{129}Xe, and ^{132}Xe were determined in a split of the DaG 489/A whole-rock sample. Apparatus and procedures are described by Loeken *et al.* (1992); results are given in Table 6; and for comparison, also those of DaG 476 (Scherer and Schultz, 1999; Zipfel *et al.*, 2000) are shown.

If it assumed that the measured ^{40}Ar is entirely of radiogenic origin, a K-Ar gas retention age of ~2.1 Ga is calculated using the K concentration of 274 ppm (Table 6). This, however, is influenced by either trapped martian, terrestrial (or both) atmospheric ^{40}Ar and possibly also by contamination of terrestrial K. With the assumption that all trapped ^{36}Ar is terrestrial contamination, the resulting K-Ar age is 0.6 Ga. It should be noted that these numbers cannot be attributed to a special event in the history of this meteorite. These numbers indicate, however, that DaG 489 has a young crystallization age similar to other members of the SNC family (except ALH 84001).

The measured ^{3}He and ^{21}Ne concentrations are taken as entirely cosmogenic. A small correction for trapped Ne ($^{20}Ne/^{22}Ne$ = 9.8) is applied to obtain the cosmogenic $^{22}Ne/^{21}Ne$ ratio that is used for the shielding correction for the production rates. Cosmogenic ^{38}Ar is obtained by assuming a mixture of trapped and cosmogenic Ar with $^{36}Ar/^{38}Ar$ = 5.00 and 0.67, respectively. This trapped value was taken because it is between the terrestrial atmospheric value of 5.32 and a possibly lower martian ratio (Bogard, 1997).

Cosmic-ray exposure ages are calculated using production rate equations and shielding corrections given by Eugster (1988). The production rates are adjusted to the chemical composition of DaG 489. Calculated ^{3}He-, ^{21}Ne-, and ^{38}Ar-exposure ages of DaG 489 and for comparison those of DaG 476 are given in Table 7. The ^{21}Ne exposure age is 1.33 Ma and is in good agreement with the ^{3}He and ^{38}Ar exposure ages of 1.03 and 1.08 Ma, respectively. We regard the ^{21}Ne exposure age as the most reliable, because ^{3}He ages are often affected by He-loss and the calculation of cosmogenic ^{38}Ar is influenced by the uncertain isotopic composition of the trapped component. The mean of the three exposure ages is 1.15 ± 0.16 Ma. This value is essentially identical to that determined for DaG 476 in the same laboratory (*i.e.*, 1.17 ± 0.09; Scherer and Schultz, 1999; Zipfel *et al.*, 2000). Although the terrestrial age of DaG 489 has not yet been measured, the typical maximum residence time of a meteorite in the Sahara desert is ~50 ka, which is in agreement with the age determined for DaG 476 of 85 ± 50 ka (Nishiizumi *et al.*, 1999). Therefore, it can be assumed that the exposure age is almost identical to the age of the ejection event at ~1.3 Ma. This is distinct from the ejection ages of all the other SNC meteorites with the exception of DaG 476 (Fig. 9). This young ejection age lends further support to the requirement of several ejection events to produce the current population of SNC meteorites.

TABLE 6. Noble gas concentrations (in 10^{-8} cm^3 STP/g) of DaG 489 and a mean of five bulk measurements of DaG 476 (Zipfel *et al.*, 2000).

Sample	^{3}He	^{4}He	^{20}Ne	^{21}Ne	^{22}Ne	^{36}Ar	^{38}Ar	^{40}Ar	^{84}Kr	^{132}Xe	$^{129}Xe/^{132}Xe$
DaG 489*	1.68	9	0.417	0.292	0.346	1.25	0.313	427	0.0467	0.0053	0.99 ±0.06
DaG 476 (mean)	1.76 ±0.21	22 ±21	0.36 ±0.02	0.26 ±0.02	0.31 ±0.02	0.95 ±0.33	0.25 ±0.07	369 ±91	0.056 ±0.019	0.012 ±0.003	0.99 ±0.01

*Uncertainties are estimated to ±5% for He, Ne, and Ar; and ±12% for Kr and Xe.

TABLE 7. Cosmogenic $(^{22}Ne/^{21}Ne)_c$, exposure ages (Ma), and K-Ar ages (Ga) for DaG 489.*

Sample	$[^{22}Ne/^{21}Ne]_c$	T3 (Ma)	T21 (Ma)	T38 (Ma)	K-Ar (Ga)
DaG 489	1.184	1.03	1.33	1.08	2.1 (0.6)
DaG 476	1.213 ± 0.012	1.09 ± 0.13	1.26 ± 0.09	1.14 ± 0.09	1.6 (0.6)

*Krypton-argon ages are calculated assuming that all ^{40}Ar is radiogenic and (given in parentheses) assuming that all ^{36}Ar is atmospheric contamination. Data from DaG 476 (Zipfel *et al.*, 2000) is given for comparison.
Uncertainties of the calculated exposure ages are estimated to be ±20%.

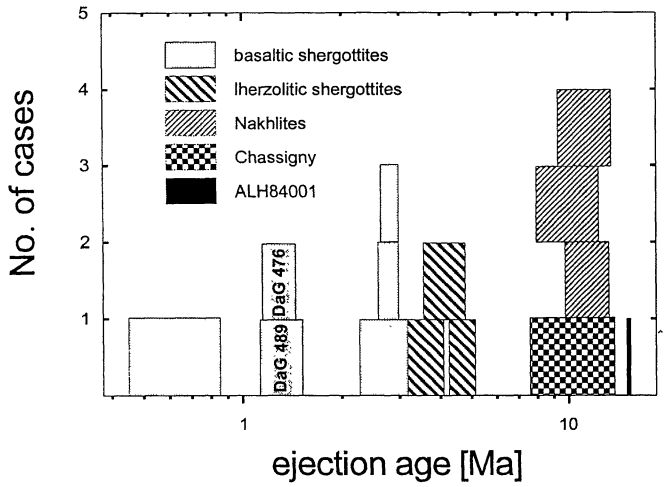

FIG. 9. Calculated ejection ages of SNC meteorites. Data from Eugster and Polnau (1997), Eugster *et al.* (1999), Nagao *et al.* (1997), and Zipfel *et al.* (2000). Boxes indicate uncertainties, including those of terrestrial ages.

Trapped martian noble gases in SNC meteorites are a mixture of martian atmospheric gas and gas from the martian mantle, represented by that measured in Chassigny (Ott, 1988). The martian atmospheric component is seen in glass inclusions, mainly from EETA79001 (*e.g.*, Garrison and Bogard, 1998). The trapped gases in DaG 489 are very similar to those in the other shergottites and in particular are virtually identical to those measured in DaG 476. The ^{84}Kr, ^{129}Xe, and ^{132}Xe systematics show that DaG 489 falls on a mixing line on a three-isotope plot between Chassigny (representative of martian mantle) and terrestrial atmosphere, indicating that no martian atmosphere has been trapped in this meteorite in detectable quantities (Fig. 10). However, Murty and Mohapatra (1999) found in a high-temperature degassing step of DaG 476 some martian atmospheric gases, characterized by a $^{129}Xe/^{132}Xe$ ratio of ~1.6. The $^{84}Kr/^{132}Xe$ ratio of 8.8 in DaG 489 reveals a high contribution of terrestrial atmospheric gases ($^{84}Kr/^{132}Xe \approx 23$) as in DaG 476 ($^{84}Kr/^{132}Xe = 4.7$). Such terrestrial atmospheric gases are commonly observed in stony meteorites from hot deserts (Scherer *et al.*, 1994) and connected to weathering products. In DaG 489, as well as in DaG 476 (Zipfel *et al.*, 2000), such products are also observed as carbonate veins that follow grain boundaries and cracks.

It is clear from the data presented in Tables 6 and 7 that the noble gas records in DaG 489 and DaG 476 are very similar. The exposure history as well as the radiogenic and trapped gases are the same within the limits of uncertainty.

HYPOTHESES ON THE PETROGENESIS OF DAR AL GANI 489

The petrographic features of DaG 489 are in part typical of basaltic shergottites, in part close to lherzolitic shergottites. The former mainly include the overall texture and modal composition; the latter include the magnesian character of the mineral constituents and the presence of abundant large olivine and chromite crystals and pyroxene with enstatitic composition. Likewise, the bulk chemical composition is on the whole intermediate between basaltic and lherzolitic shergottites, although closer to the latter. This hybrid character suggests some relationship between the two shergottite subgroups.

Furthermore, DaG 489 is similar to the hybrid shergottite EETA79001 lithology A and identical to DaG 476, in terms of petrography and bulk chemistry. In particular, a common feature to all three meteorites are their three-pyroxene assemblages, which suggest a complex crystallization history, and the lherzolite-like assemblage of olivine, chromite, and enstatite that show corrosion microstructures (although to various extent) indicative of disequilibrium interaction with the surrounding basaltic melt. Nonetheless, some relevant differences are observed between DaG 489/DaG 476 and EETA79001 lithology A: DaG 489 and DaG 476 have a higher olivine content (~20 vol%); lack of orthopyroxene megacrysts; contain Mg-richer pigeonite, augite, and oxides; and have a higher molar (Mg/Mg + Fe) = 0.68 and a lower REE content in the bulk sample. Therefore, DaG 489 and DaG 476 have the potential of providing us with a further petrogenetic link between basaltic and lherzolitic shergottites.

Indeed, the similarity of DaG 489 and DaG 476 with EETA79001 lithology A points to a similar petrogenesis. Three hypotheses have been formulated for the origin of EETA79001 lithology A: (1) hybrid rock originated by incorporation and partial assimilation of lherzolitic material by a basaltic melt (*e.g.*, McSween and Jarosewich, 1983); (2) hybrid rock originated by mixing between a lherzolitic and a basaltic melt (*e.g.*, Wadhwa *et al.*, 1994); (3) impact melting of a basalt plus lherzolite target (Mittlefehldt *et al.*, 1999).

For the petrogenesis of DaG 476, Zipfel *et al.* (2000) reevaluated possibilities (1–3) and discussed two additional hypotheses: (4) closed-system crystallization of a highly magnesian melt (shergottite parent magma or impact melt) having a DaG 476 bulk-rock composition; and (5) cumulate rock formed by the accumulation of olivine, enstatite, and chromite primocrysts into a

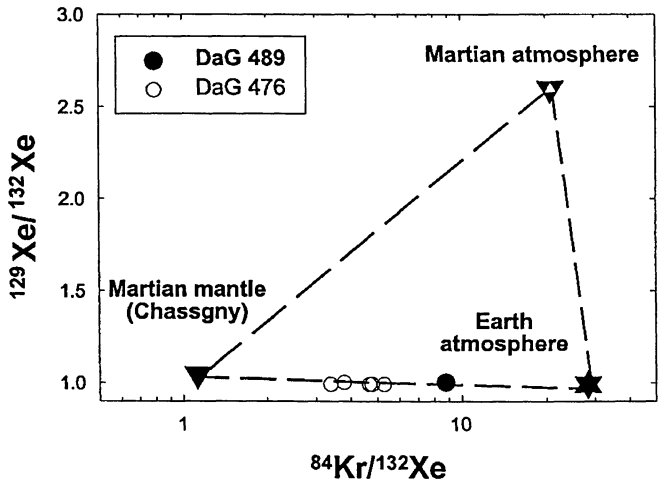

FIG. 10. Three-isotope plot of $^{129}Xe/^{132}Xe$ *vs.* $^{84}Kr/^{132}Xe$. The DaG 489 measurement (full symbol) as well as those of DaG 476 lie on the mixing line between martian mantle gas (Chassigny) and the terrestrial atmosphere. This indicates that both Dar al Gani SNC meteorites contain appreciable amounts of trapped Kr and Xe from the terrestrial atmosphere.

shergottite parent magma. They concluded that hypotheses (2) and (5) can be ruled out and that hypothesis (4) is the most viable.

In addition to those listed above, we tentatively propose a sixth hypothesis for the origin of DaG 489, which accounts for the textural, microstructural, and compositional characteristics of the olivine–chromite–enstatite assemblage, and for the close geochemical affinity to lherzolitic shergottites: (6) high-degree partial melting of a lherzolite-like material, followed by segregation of a melt that entrains a fraction of unmelted phases. Dar al Gani 489 might in fact be a "crystal mush": the high-temperature assemblage given by the magnesian olivine cores, the enstatitic cores to pigeonite crystals, and the large chromite crystals would represent partial melting residues, disaggregated, and interspersed in the melt fraction given by the basaltic (pigeonite and feldspathic glass) groundmass.

This hypothesis has been tested by means of major element mass balance, assuming that the DaG 489 source rock is akin to known martian lherzolites. A bulk composition very close to that of DaG 489 can be obtained by subtracting a residue consisting of olivine, enstatite, and Cr-rich spinel with the same compositions as those found in DaG 489 from the average composition of Y-793605, ALH 77005, and LEW 88516 (Fig. 11, Table 8). The results of the least-squares calculation indicate that DaG 489 represents 58 wt% of the initial mass. As the proportion of unmelted phases in DaG 489 was estimated to be 27 wt% of the bulk rock (Table 1), this implies that the melt represents 42 wt% of the initial lherzolite-like source, all of which remains with the "crystal mush." These figures are in agreement with the incompatible trace element distribution of DaG 489. Indeed, a rock consisting of a high-degree melt plus unmelted source phases should have: (1) an incompatible trace element distribution matching that of the initial source and (2) incompatible trace element concentrations slightly higher than the source. Therefore, the extreme LREE depletion of DaG 489 could reflect an equally, or more, LREE-depleted source, like the lherzolitic

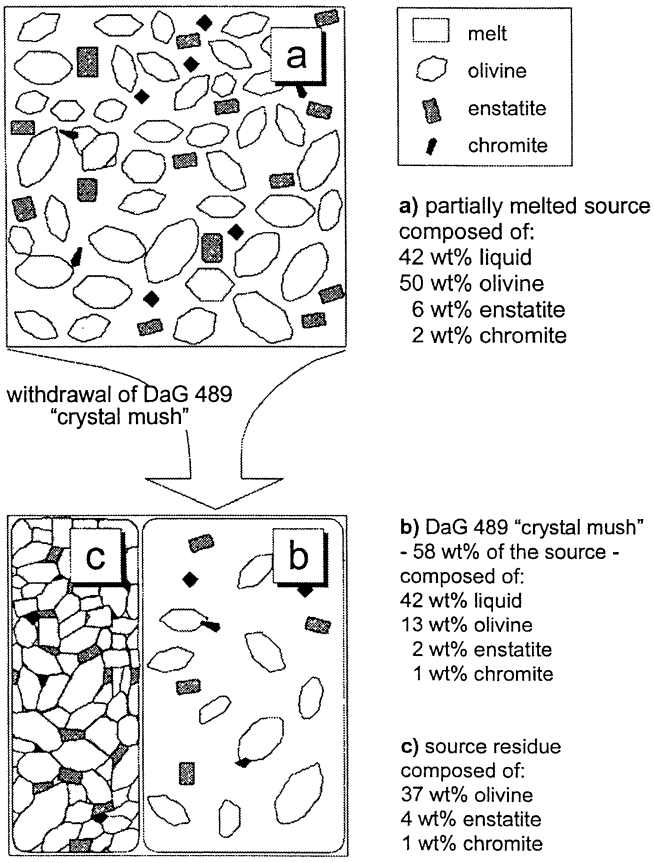

FIG. 11. Schematic illustrating the origin of DaG 489 through high-degree partial melting of a lherzolite-like material, followed by segregation of a melt that entrains a fraction of unmelted phases. See text for explanation.

TABLE 8. Mass-balance modelling for the origin of DaG 489.*

	Source†	DaG 489‡	Residual source phases			Model composition
			Olivine§	Enstatite#	Cr-spinel$	
SiO_2	44.7	49.7	37.9	55.0	–	49.3
TiO_2	0.4	0.4	–	–	6.9	0.6
Al_2O_3	2.6	4.4	–	0.7	9.2	4.3
FeO_{tot}	19.7	17.2	24.8	12.9	35.8	16.6
MnO	0.5	0.4	0.6	0.4	0.5	0.4
MgO	26.5	20.2	36.4	28.7	4.6	20.4
CaO	3.8	5.9	0.2	1.5	–	6.4
Na_2O	0.4	0.6	–	–	–	0.7
K_2O	0.03	0.03	–	–	–	0.04
P_2O_5	0.4	0.5	–	–	–	0.7
Cr_2O_3	0.9	0.7	–	0.6	43.0	0.6
Source residue (wt%) after extraction of DaG 489 "crystal mush"			–37.2	–4.3	–1.2	

*Through high-degree partial melting of a lherzolite-like material, followed by segregation of a melt that entrains a fraction of unmelted phases. See text for a more detailed explanation.
†Average composition of the lherzolitic shergottites Y-793605 (Warren and Kallemeyn, 1997), ALH 77005, and LEW 88516 (Dreibus *et al.*, 1992).
‡Content of CaO corrected on the assumption that DaG 489 contains the same amount of secondary $CaCO_3$ (3.9 wt%) as DaG 476 does (Zipfel *et al.*, 2000).
§Average composition ($n = 7$) of cores of olivine crystals >500 μm from DaG 489.
#Average composition ($n = 9$) of blocky enstatite cores from DaG 489.
$Average composition ($n = 35$) of Cr-rich spinel crystals from DaG 489.
All analyses recalculated to 100%.

shergottite Y-793605 (Ebihara *et al.*, 1997) or the potential source of the basaltic shergottite QUE 94201 (McSween *et al.*, 1996). Alternatively, DaG 489 may represent an *in situ* partial melting of a lherzolite-like source rock with DaG 489 bulk composition. In this latter case, the degree of melting would be as high as 73 wt% of the initial source. In both cases, the homogeneous dispersion of the unmelted phases could be primarily due to the high degree of melting and complete disruption of the initial source. Impact processes might have provided the necessary heat to reach such high degrees of partial melting, as already suggested by Mittlefehldt *et al.* (1999) for the impact-melt origin (hypothesis (3)) of EETA79001 lithology A.

DAR AL GANI 489 PAIRED WITH DAR AL GANI 476

Both DaG 489 and DaG 476 have quite distinctive petrographic and mineralogical features, bulk chemistry, and exposure history compared to the other SNC meteorites. That two such rare and identical meteorites were found 25 km apart in the Dar al Gani desert (Fig. 2) strongly suggests that they are fragments of the same fall.

As fragmentation during atmospheric flight usually produces many fragments (*e.g.*, Halliday *et al.*, 1991), it is possible that additional pieces of this fall rest on the Dar al Gani desert.

Studies of strewnfields of shower falls (*e.g.*, Bevan *et al.*, 1998) indicate that, in general, masses are distributed in ellipses and are sorted by weight along its major axis, with the larger masses pointing at the direction of flight. Because DaG 489 and DaG 476 weigh about the same (2146 and 2015 g, respectively), one may speculate that any possible strewnfield of this fall trends east-west (Fig. 2) (*i.e.*, normal to the line tying their find locations). This argument would hold assuming a simple fragmentation history and that both fragments were found where they fell, that is, that no mass-transport, either exogenic or anthropogenic, occurred since their fall.

CONCLUSIONS

(1) Petrographic data, bulk chemical composition, and O-isotopic compositions confirm previous report (Grossman, 1999; Folco *et al.*, 1999) indicating that DaG 489 is martian and can be classified as a highly shocked (shock stage ≥S5), basaltic shergottite.

(2) Petrographic data and bulk chemical composition show that DaG 489 is similar to the hybrid shergottite EETA79001 lithology A. However, the petrography and bulk chemistry of DaG 489 is somewhat distinct from EETA79001 lithology A, and thus DaG 489 provides us with a further petrogenetic link between basaltic and lherzolitic shergottites.

(3) Noble gas analyses show that DaG 489 has an ejection age of ~1.3 Ma. This young age lends support to the requirement of several ejection events to produce the current population of SNC meteorites.

(4) Petrographic and bulk chemical data, noble gases inventory, and find locations are consistent with DaG 489 being paired with DaG 476.

(5) In addition to the existing hypotheses on the petrogenesis of the similar EETA79001 lithology A and the identical DaG 476, we propose that DaG 489 could have formed through high-degree partial melting of a lherzolite-like source material.

Acknowledgements–The finder of DaG 489 is thanked for providing us with details of the find, for allowing us the inspection of the whole meteorite, and for donating samples to the Museo Nazionale dell'Antartide of the University of Siena (MNA-SI) for research. Filippo Olmi is thanked for assistance with EMP analyses at the CNR-CSMGA laboratories in Florence. Bulk chemical analyses were carried out at the Dipartimento Scienze della Terra of the University of Pisa; Marco Tamponi and Marco Bertoli are acknowledged for their help in the bulk chemical analyses at the Dipartimento di Scienze della Terra of the University of Pisa; the ICP-MS and clean lab facilities were funded by G. N. V. and the Italian Antarctic Research Programme (PNRA). Arabelle S. Sexton is thanked for assistance with O-isotopic analyses at the Planetary Sciences Research Institute of the Open University (PSRI-OU). PNRA provided financial support. Jutta Zipfel and Takashi Mikouchi are thanked for thorough reviews, and Ed Scott for editorial assistance.

Editorial handling: E. R. D. Scott

REFERENCES

BECKER R. H. AND PEPIN R. O. (1984) The case for the martian origin of the shergottites: Nitrogen and noble gases in EETA79001. *Earth Planet. Sci. Lett.* **69,** 225–242.

BECKER R. H. AND PEPIN R. O. (1986) Nitrogen and light noble gases in Shergotty. *Geochim. Cosmochim. Acta* **50,** 993–1000.

BENCE A. E. AND ALBEE A. L. (1968) Empirical correction factors for the electron microanalysis of silicates and oxides. *J. Geol.* **76,** 382–403.

BEVAN A. W. R., BLAND P. A. AND JULL J. T. (1998) Meteorite flux on the Nullarbor Region, Australia. In *Meteorites: Flux with Time and Impact Effects* (eds. M. M. Grady, R. Hutchison, G. J. H. McCall and D. A. Rothery), pp. 59–73. Geol. Soc. Spec. Publ. **140,** Geol. Soc., London, U.K.

BISCHOFF A. *ET AL.* (1998) Petrology, chemistry, and isotopic compositions of the lunar highland regolith breccia Dar al Gani 262. *Meteorit. Planet. Sci.* **33,** 1243–1257.

BOGARD D. D. (1997) A reappraisal of the Martian $^{36}Ar/^{38}Ar$ ratio. *J. Gephys. Res.* **102,** 1653–1661.

BOGARD D. D. AND JOHNSON P. (1983) Martian gases in an Antarctic meteorite. *Science* **221,** 651–654.

BOGARD D. D., NYQUIST L. E. AND JOHNSON P. (1984) Noble gas contents of shergottites and implications for the Martian origin of SNC meteorites. *Geochim. Cosmochim. Acta* **48,** 1723–1739.

BURGHELE A., DREIBUS G., PALME H., RAMMENSEE W., SPETTEL B., WECKWERTH G. AND WÄNKE H. (1983) Chemistry of shergottites and the shergottite parent body (SPB): Further evidence for the two components model for planet formation (abstract). *Lunar Planet. Sci.* **14,** 80–81.

D'ORAZIO M. AND TONARINI S. (1997) Simultaneous determination of neodymium and samarium in silicate rocks and minerals by isotope dilution inductively coupled plasma mass spectrometry: Results on twenty geochemical reference samples. *Anal. Chim. Acta* **351,** 325–335.

DREIBUS G., JOCHUM K. P., PALME H., SPETTEL B., WLOTZKA F. AND WÄNKE H. (1992) LEW 88516: A meteorite compositionally close to the "Martian mantle" (abstract). *Meteoritics* **27,** 216–217.

DREIBUS G., SPETTEL B., WLOTZKA F., SCHULTZ L., WEBER H. W., JOCHUM K. P. AND WÄNKE H. (1996) QUE 94201: An unusual Martian basalt (abstract). *Meteorit. Planet. Sci.* **31 (Suppl.),** A39–A40.

EBIHARA M., KONG P. AND SHINOTSUKA K. (1997) Chemical composition of Y-793605, a Martian lherzolite. *Antarctic Meteorite Research* **10,** 83–94.

EUGSTER O. (1988) Cosmic-ray-production rates for ^{3}He, ^{21}Ne, ^{38}Ar, ^{83}Kr, and ^{126}Xe in chondrites based on ^{81}Kr-Kr exposure ages. *Geochim. Cosmochim. Acta* **52,** 1649–1659.

EUGSTER O. AND POLNAU E. (1997) Mars–Earth transfer time of lherzolite Yamato 793605. *Antarctic Meteorite Research* **10,** 143–149.

EUGSTER O., WEIGEL A. AND POLNAU E. (1999) Ejection times of Martian meteorites. *Geochim. Cosmochim. Acta* **61,** 2749–2757.

FOLCO L., FRANCHI I. A., SCHERER P., SCHULTZ L. AND PILLINGER C. T. (1999) Dar al Gani 489 basaltic shergottite: A new find from the Sahara likely paired with Dar al Gani 476 (abstract). *Meteorit. Planet. Sci.* **34 (Suppl.),** A36–A37.

FRANCHI I. A., WRIGHT I. P., SEXTON A. S. AND PILLINGER C. T. (1999) The oxygen isotopic composition of Earth and Mars. *Meteorit. Planet. Sci.* **34,** 657–661.

GARRISON D. H. AND BOGARD D. D. (1998) Isotopic composition of trapped and cosmogenic noble gases in several Martian meteorites. *Meteorit. Planet. Sci.* **33,** 721–736.

GROSSMAN J. N. (1999) The Meteoritical Bulletin No. 83, 1999 July. *Meteorit. Planet. Sci.* **34 (Suppl.),** A169–A186.

HALLIDAY I., BLACKWELL A. T. AND GRIFFIN A. A. (1991) The frequency of meteorite falls: Comments on two conflicting solutions to the problem. *Meteoritics* **26,** 243–249.

HARVEY R. P., WADHWA M., MCSWEEN H. Y., JR. AND CROZAZ G. (1993) Petrography, mineral chemistry, and petrogenesis of Antarctic Shergottite LEW 88516. *Geochim. Cosmochim. Acta* **57,** 4769–4783.

HOEFS J. (1997) *Stable Isotope Geochemistry*. Springer-Verlag, Berlin, Germany. 201 pp.

IKEDA Y. (1994) Petrography and petrology of the ALH 77005 shergottite. *Proc. NIPR Symp. Antarct. Meteorites* **7,** 9–29.

IKEDA Y. (1997) Petrology and mineralogy of the Y-793605 Martian meteorite. *Antarctic Meteorite Research* **10,** 13–40.

LAUL J. C., SMITH M. R., WÄNKE H., JAGOUTZ E., DREIBUS G., PALME H., SPETTEL B., BURGHELE A., LIPSCHUTZ M. E. AND VERKOUTEREN R. M. (1986) Chemical systematics of the Shergotty meteorite and the composition of its parent body (Mars). *Geochim. Cosmochim. Acta* **50,** 909–926.

LE MAITRE R. W., ED. (1989) *A Classification of Igneous Rocks and Glossary of Terms*. Blackwell Scientific Publications, Oxford, U.K. 193 pp.

LOEKEN T., SCHERER O., WEBER H. W. AND SCHULTZ L. (1992) Noble gases in eighteen stone meteorites. *Chem. Erde* **52,** 249–259.

MCDONOUGH W. F. AND SUN S-S. (1995) The composition of the Earth. *Chem. Geol.* **120,** 223–253.

MCSWEEN H. Y., JR. (1994). What we have learned about Mars from SNC meteorites. *Meteoritics* **29,** 757–779.

MCSWEEN H. Y., JR. AND JAROSEWICH E. (1983) Petrogenesis of Elephant Moraine A79001 meteorite: Multiple magma pulses on the shergottite parent body. *Geochim. Cosmochim. Acta* **47,** 1501–1513.

MCSWEEN H. Y., JR. AND TREIMAN A. H. (1998) Martian meteorites. In *Planetary Materials* (ed. J. J. Papike), pp. 6-01–6-53. Rev. Mineral. **36,** Mineral. Soc. America, Washington, D.C., USA.

MCSWEEN H. Y., JR., TAYLOR L. A. AND STOLPER E. (1979) Allan Hills 77005: A new meteorite type found in Antarctica. *Science* **204,** 1201–1203.

McSween H. Y., Jr., Eisenhour D. D., Taylor L. A., Wadhwa M. and Crozaz G. (1996) QUE 94201 shergottite: Crystallization of a Martian basaltic magma. *Geochim. Cosmochim. Acta* **60,** 4563–4569.

Mikouchi T. (1999) Preliminary examination of Dar al Gani 476: A new basaltic Martian meteorite similar to lithology A of EETA79001 (abstract). *Lunar Planet. Sci.* **30,** #1557, Lunar and Planetary Institute, Houston, Texas, USA (CD-ROM).

Mikouchi T. and Miyamoto M. (1997) Yamato-793605: A new lherzolitic shergottite from the Japanese Antarctic meteorite collection. *Antarctic Meteorite Research* **10,** 41–60.

Mikouchi T., Miyamoto M. and McKay G. A. (1998) Mineralogy of Antarctic basaltic shergottite Queen Alexandra Range 94201: Similarities to Elephant Moraine A79001 (Lithology B) Martian meteorite. *Meteorit. Planet. Sci.* **33,** 181–189.

Miller M. F., Franchi I. A., Sexton A. S. and Pillinger C. T. (1999) High precision $\delta^{17}O$ isotope measurements of oxygen from silicates and other oxides: Method and applications. *Rapid Comm. Mass Spec.* **13,** 1211–1217.

Mittlefehldt D. W., Lindstrom D. J., Lindstrom M. M. and Martinez R. R. (1999) An impact-melt origin for lithology A of Martian meteorite Elephant Moraine A79001. *Meteorit. Planet. Sci.* **34,** 357–367.

Mittlefehldt D. W., Wentworth S. J., Wang M-S., Lindstrom M. M. and Lipschutz M. E. (1997) Geochemistry of and alteration phases in Martian lherzolite Y-793605. *Ant. Met. Res.* **10,** 109–124.

Morimoto N. (1988) Nomenclature of pyroxenes. *Am. Mineral.* **73,** 1123–1133.

Murty S. V. S. and Mohapatra R. K. (1999) Cosmogenic and trapped components in the Martian meteorite Dar al Gani 476 from hot desert. In *Workshop on Extraterrestrial Materials from Cold and Hot Deserts* (eds. L. Schultz, I. Franchi, A. Reid and M. Zolensky), pp. 57–60. LPI Tech. Rep. #997, Lunar and Planetary Institute, Houston, Texas, USA.

Nagao K., Nakamura T., Miura Y. N. and Takaoka N. (1997) Noble gases and mineralogy of primary igneous materials in the Yamato 793605 shergottite. *Ant. Met. Res.* **10,** 125–142.

Nishiizumi K., Masarik J., Welten K. C. Caffee M. W., Jull A. J. T. and Klandrud S. E. (1999) Exposure history of new Martian meteorite Dar al Gani 476 (abstract). *Lunar Planet. Sci.* **30,** #1966, Lunar and Planetary Institute, Houston, Texas, USA (CD-ROM).

Ott U. (1988) Noble gases in SNC meteorites: Shergotty, Nakhla, Chasssigny. *Geochim. Cosmochim. Acta* **52,** 1937–1948.

Papike J. J. (1998) Comparative planetary mineralogy: Chemistry of melt-derived pyroxene, feldspar, and olivine. In *Planetary materials* (ed. J. J. Papike), pp. 7-01–7-11. Rev. Mineral. **36,** Mineral. Soc. America, Washington, D.C., USA

Scherer P. and Schultz L. (1999) Noble gases in the SNC meteorite Dar al Gani 476 (abstract). *Lunar Planet. Sci.* **30,** #1144, Lunar and Planetary Institute, Houston, Texas, USA (CD-ROM).

Scherer P., Schultz L. and Loeken T. (1994) Weathering and atmospheric noble gases in chondrites. In *Noble Gas Geochemistry and Cosmochemistry* (ed. J. Matsuda), pp. 43–53. Terra Sci. Publ. Co., Tokyo, Japan.

Shih C-Y., Nyquist L. E., Bogard D. D., McKay G. A., Wooden J. L., Bansal B. M. and Wiesmann H. (1982) Chronology and petrogenesis of young achondrites, Shergotty, Zagami, and ALHA77005: Late magmatism on a geologically active planet. *Geochim. Cosmochim. Acta* **46,** 2323–2344.

Smith M. R., Laul J. C., Ma M-S., Huston T., Verkouteren R. M., Lipschutz M. E. and Schmitt R. A. (1984) Petrogenesis of the SNC (shergottites, nakhlites, chassignites) meteorites: Implications for their origin from large, dynamic planet, possibly Mars. *Proc. Lunar Planet Sci. Conf.* **14th,** *J. Geophys. Res.* **89 (Suppl.),** B612–B630.

Steele I. M. and Smith J. V. (1982) Petrography and mineralogy of two basalts and olivine-pyroxene-spinel fragments in achondrite EETA79001. *J. Geophys. Res.* **87 (Suppl.),** A375–A384.

Stöffler D., Keil K. and Scott R. D. (1991) Shock metamorphism of ordinary chondrites. *Geochim. Cosmochim. Acta* **55,** 3845–3867.

Stolper E. M. and McSween H. Y., Jr. (1979) Petrology and origin of the shergottite meteorites. *Geochim. Cosmochim. Acta* **43,** 1475–1498.

Swindle T. D., Caffee M. W. and Hohenberg C. M. (1986) Xenon and other noble gases in shergottites. *Geochim. Cosmochim. Acta* **50,** 1001–1015.

Treiman A. H., Drake M. J., Janssens M-J., Wolf R. and Ebihara M. (1986) Core formation in the Earth and the Shergottite Parent Body (SPB): Chemical evidence from basalts. *Geochim. Cosmochim. Acta* **50,** 1071–1091.

Wadhwa M., McSween H. Y., Jr. and Crozaz G. (1994). Petrogenesis of shergottite meteorites inferred from minor and trace element micro-distributions. *Geochim. Cosmochim. Acta* **58,** 4213–4229.

Warren P. H. and Kallemeyn G. W. (1997) Yamato-793605, EET79001 and other presumed Martian meteorites: Compositional clues to their origins. *Ant. Met. Res.* **10,** 61–81.

Wiens R. C., Becker R. H. and Pepin R. O. (1986) The case for a martian origin of the shergottites. II. Trapped and indigenous gas components in EETA79001 glass. *Earth Planet. Sci. Lett.* **77,** 149–158.

Zipfel J., Spettel B., Palme H. and Dreibus G. (1999) Petrology and chemistry of Dar al Gani 476, A new basaltic Shergottite (abstract). *Lunar Planet. Sci.* **30,** #1206, Lunar and Planetary Institute, Houston, Texas, USA (CD-ROM).

Zipfel J., Scherer P., Spettel B., Dreibus G. and Schultz L. (2000) Petrology and chemistry of the new shergottite Dar al Gani 476. *Meteorit. Planet. Sci.* **35,** 107–115.